

Investigation of Thin Film Flow on a Stretching Cylinder in Unsteady Motion with variable Heat Source/Sink

Pradeep G. Janthe¹ and Jagadish V Tawade^{2,*}

^{1,2}Department of Mathematics, Vishwakarma University, Pune-411048, India.

¹pradeepjanthe@gmail.com ; ²jagadish.tawade@vupune.ac.in

Corresponding authors: Email: jagadish.tawade@vupune.ac.in (Jagadish V. Tawade)

Article History:

Received: 31-07-2024

Revised: 20-09-2024

Accepted: 30-09-2024

Abstract:

In this study, we explore the effects of momentum and heat transfer in a thin liquid film over a cylinder that is stretched and undergoes unsteady motion, with the impact of a magnetic field and a non-uniform heat source/sink. Through the use of similarity transformations, the complex system of PDEs (Partial differential equations) is transformed into the ODEs (Ordinary differential equations). This process involves manipulating the equations in such a way that they can be simplified into a set of ODEs, which are typically easier to solve and analyze. By applying these transformations, the system becomes more manageable and can be studied more effectively. Using the `bvp4c` function in MATLAB which was provided a powerful tool for solving boundary value problems (BVPs) efficiently, particularly when dealing with systems of ODEs. This function utilizes a robust algorithm to numerically solve the ODE system while considering the specified boundary conditions. Graphs are frequently utilized to visually illustrate the effects of different parameters on temperature and velocity profiles in the presence of a variable heat source/sink and an external magnetic field. When the magnetic parameter increases, we observe that the decrease in the velocity profile and film thickness of the fluid and also Heat source/sink parameters lead to fluid temperature enrichment.

Keywords: Thin film, unsteady flow, external magnetic field, Stretching cylinder, boundary value problems.

1. Introduction:

In recent decades, analysts have extensively studied the flow of heat transfer because their significant applications in modern engineering. For the purpose of researching the covering process and developing heat transfers and chemical apparatus, it is essential to comprehend the heat and mass transfer inside the thin fluid layer. It also has numerous applications in modern engineering processes, such as in paper production, materials created through the extrusion process, the fluid film's boundary layer in the solidification scheme, food processing, cable insulation, Maintaining the temperature of metal sheets, streamlined extrusion of plastic sheet, polymer coatings, and hot rolling, strengthening and copper wires coating. Studying the transfer of heat across a stretched surface in a fluid nearby is currently a major area of interest for researchers. Figure 1 is the schematic representation of the physical model for the thin liquid film over a stretching cylinder. This topic has wide-ranging applications in various scientific and engineering fields, particularly in chemical engineering. For example, it is relevant in areas such as metallurgy and polymer moulding, where the heat exchange

systems are included in the liquid melt's condensation process. In these processes, stretching rate and heat exchange have the greatest effects on the final product's rheological characteristics. For example, during synthetic fibre processing, the material undergoes extrusion from a die, resulting in the formation of long strands or filaments. These strands are then condensed through gradual cooling.

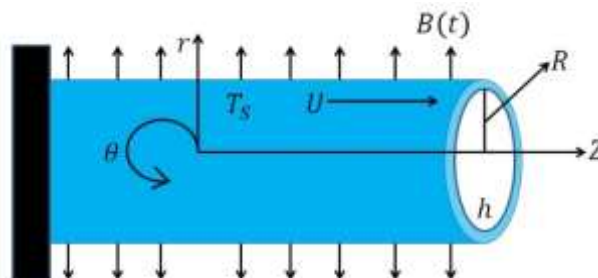


Figure 1. Schematic representation of the physical model

Gogoi and Maity [1] explores the thermocapillary effect is on the thin-film flow upon a porous stretching cylinder. Alabdulhadi et. Al. [2] their study investigates heat transmission and Unsteady thin-film flow consisting of Al_2O_3 nanoparticles dispersed in water across an inclined stretched surface, considering the impact of buoyancy force. Zhang et. Al. [3] studied Thermosolutal Capillarity and Magnetic Field Affect Heat and Mass Transfer in the Thin Liquid Film Over a Moving Surface. Vajravelu et al. [4] explores variation of the thermal conductivity and the viscous dissipation with the temperature on unsteady flow and heat transfer of the non-Newtonian Ostwald-de Waele fluid. The fluid is spread as a thin liquid layer across a horizontal porous stretched surface.

Ziad Khan et. al. [5] explore about the hybrid nanofluid stagnation point flow's radiation heat transfers via a porous cylinder that is stretching. Hayat et. Al. [6] examined the flow of thin films and ways to enhance heat transfer by dispersing copper nanoparticles in ethylene glycol. Shahazad et. Al. [7] examined using numbers of axisymmetric flow and the heat transmission in liquid layer over the surface that is extending radially with time-varying properties. Khan W and Gul T [8] conducted an analysis of the ability of boundary layer flow to shield an unstable cylinder's surface from outside heating and cooling while taking non-Newtonian Walter's B fluid into consideration.

Mostafa and Megahed [9] investigated the Heat transmission and MHD flow in non-Newtonian liquid layer over the unstable stretched sheet with the variable fluid characteristics. Waheed [10] investigated the Heat transmission and flow through the Maxwell liquid layer on the unsteady stretched sheet in radiation-containing the porous medium. Kandwal et. Al. [11] explored effect of suction/injection and the viscous dissipation on numerical study of nanofluid heat transmission in stretched cylinder. Gomathy & Rushi Kumar [12] conducted an examination of the intricate dynamics of heat transmission and thin-film flow in porous media, with an emphasis on the behaviour of Al_2O_3 nanoparticles in relation to their form. Tawade et. Al. [13] explored the computational analysis of the Casson nanofluid flow via porous materials on stretching magnetic surfaces. Gamal and Abdel-Rahman [14] studied the Influence of Magnetohydrodynamics on Unsteady Micropolar Fluid Thin Films via a Porous Media.

Alshehry et. Al. [15] explored the thin-film nanofluids heat flow on an inclined disc using HWCM. Govindasamy [16] examined the thin-film flow of Casson nanofluid across an unstable stretching sheet, and observed that impact on heat and mass transport. Ali and Alim [17] studied about heat flow

and the boundary layer flow through bullet-shaped object that is both stretched and unstretched by numerically. Jawad et al. [18] focuses on flow of thin layer of MHD nanofluid, taking into account the special effects of Navier's partial slip, Darcy-Forchheimer flow and Joule dissipation. Hayat [19] carried out a numerical investigation on increase of thin film flow and heat transfer for the copper nanoparticles distributed within the ethylene glycol. Yan Zhang [20] studied the impact of slip velocity, Power-law and unstable magnetic field over the stretched sheet. Miran and Sohn [21] explored a numerical analysis of curved edges on the flow around the square cylinder.

Shahzad et al. [22] explored the flow and heat transmission in the thin layer along an unstable stretched cylinder are analysed numerically. Anantha et al. [23] Studied the impact of a non-uniform heat source/sink on MHD hybrid ferrofluid's radiative thin-film flow. Giri et al. [24] examine the consequences on heat transmission and unstable nanofluid flow in the finite thin layer with the non-uniform heat source/sink. Khan et al. [25] as studied A stretched cylinder with heat transfer was sprayed with a magnetohydrodynamic thin film nanofluid. Hayat et al. [26] studied the analytically determined flow of a fourth-grade fluid down a vertical cylinder. Ross et al. [27] studied the Viscoplastic Material's flow of Thin-Film Around the Big Horizontal Stationary or Rotating Cylinder.

According to the literature survey, there have been no previous attempts to investigate the thermos-physical Fluid motion in a liquid film flowing across a cylinder that may be stretched. The problem becomes more complex as the cylinder stretches and the liquid film is involved. This current investigation aims to address the need for a dependable Numerical technique for solving liquid film problems over stretched surfaces.

2. Mathematical formulation:

We examine a stretchable cylinder of the radius R that is covered in the thin layer of viscous fluid with thickness h , fig. 1. The motion in the fluid which is caused by the stretching cylinder along the z -direction of the coordinate system. Surface velocity $U(z, t) = \frac{bz}{(1-\alpha_1 t)}$, Here b and α_1 are positive and dimension $[t^{-1}]$, $T = T_s = T_0 - T_{ref}(bz^2/2\nu)(1 - \alpha_1 t)^{-3/2}$ is the stretching cylinder temperature, T_0 is the temperature at the slit and reference temperature is T_{ref} which is constant. The velocity $U(z, t)$ of stretching cylinder emulates the rate $b/(1 - \alpha_1 t)$ is rises with the time. $T_s(z, t)$ is the surface temperature of the cylinder; it shows that over time, the temperature falls along the cylinder starting at T_0 at the slit and decreasing in proportion to z^2 .

The $B(t) = [B_0(t)/(1 - \alpha_1 t)^{1/2}]$ is uniform magnetic field is directed radially. By selecting the expressions $U(z, t)$, $T_s(z, t)$, $B(r, t)$, we can construct new similarity transformations that will convert the momentum and heat equation's governing PDEs into the ODEs system.

The q''' is heat source/sink which is non-uniform, given by

$$q''' = \frac{kU}{x\vartheta} [A^*(T_w - T_0) + B^*(T_w - T_0)]$$

Here, the varying in A^* and B^* which represents the internal heat source and sink, respectively.

By analyzing the movement of a fluid that cannot be compressed and has a high resistance to flow around a stretching cylinder, we can determine the equations governing motion and heat transfer. The equation that governs the velocity and temperature field in a two-dimensional boundary layer:

$$\frac{\partial}{\partial r}(ru) + \frac{\partial}{\partial z}(rw) = 0 \quad (1)$$

$$\frac{\partial w}{\partial t} + u \frac{\partial w}{\partial r} + w \frac{\partial w}{\partial z} = \nu \left[\frac{1}{r} \frac{\partial}{\partial r} \left(r \frac{\partial w}{\partial r} \right) \right] - \frac{\sigma B^2}{\rho(1 - \alpha_1 t)} w \quad (2)$$

$$\frac{\partial T}{\partial t} + u \frac{\partial T}{\partial r} + w \frac{\partial T}{\partial z} = \frac{\nu}{C_p} \left(\frac{\partial w}{\partial r} \right)^2 + \alpha \left[\frac{1}{r} \frac{\partial}{\partial r} \left(r \frac{\partial T}{\partial r} \right) \right] + \frac{q'''}{\rho C_p} \quad (3)$$

The above eq's consider the velocity field to be $\vec{v} = [u(r, t, z), 0, w(r, t, z)]$, The radial velocity is denoted by u while the axial velocity is denoted by w . $\nu = \mu/\rho$ – kinematic viscosity, μ – viscosity coefficient of a fluid, ρ – density of fluid, T – fluid temperature and $\alpha = \frac{k}{\rho C_p}$ – fluid's thermal diffusivity.

The following are the boundary conditions:

$$\left. \begin{aligned} w = U(z) = \frac{bz}{(1 - \alpha_1 t)}, \quad u = 0, T = T_s \quad \text{at } r = R \\ \frac{\partial w}{\partial r} = 0, \frac{\partial T}{\partial r} = 0, u = \frac{dh}{dt} \quad \text{at } r = R + h \end{aligned} \right\} \quad (4)$$

The similarity variables are as follows:

$$\psi = (U\nu z)^{\frac{1}{2}} R f(\eta), \eta = \frac{r^2 - R^2}{2R} \left(\frac{U}{\nu z} \right)^{\frac{1}{2}}, \quad \theta(\eta) = \frac{T - T_0}{-T_{ref} \left(\frac{bz^2}{2\nu} \right) (1 - \alpha_1 t)^{-\frac{3}{2}}} \quad (5)$$

Here, non-dimensional temperature θ and independent variable η . Then Stream function is $\psi(r, z)$:

$$u = -\frac{1}{r} \frac{\partial \psi}{\partial z}, w = \frac{1}{r} \frac{\partial \psi}{\partial r} \quad (6)$$

u and w , are velocity components, may be expressed as follows:

$$u = -\frac{r}{R} \left(\frac{bv}{1 - \alpha_1 t} \right)^{\frac{1}{2}} f(\eta), w = \frac{bz}{(1 - \alpha_1 t)} f' \quad (7)$$

The definition of the stream function properly satisfies the continuity equation. Equations (2) and (3), with eq. (4) substituted, provide the following governing equations and boundary conditions (4):

$$(1 + 2C\eta)f''' + 2Cf'' - (M + S)f' - \frac{S\eta}{2}f'' + ff'' - (f')^2 = 0 \quad (8)$$

$$(1 + 2C\eta)\theta'' + 2C\theta' + Pr \left[f\theta' - 2f'\theta - \frac{S}{2}(3\theta + \eta\theta') + (A^*f' + B^*\theta) + Ec(1 + 2C\eta)f''^2 \right] = 0 \quad (9)$$

$$\left. \begin{aligned} f(0) = 0, f'(0) = \theta(0) = 1 \\ f''(\beta) = \theta'(\beta) = 0, f(\beta) = \frac{S\beta}{2} \end{aligned} \right\} \quad (10)$$

In the non-dimensional equations. (8) and (9), $\beta = [h + (h^2/2R)]\{b/[(1 - \alpha_1 t)v]\}^{1/2}$ is dimensionless film thickness, $C = \{[(1 - \alpha_1 t)v]/bR^2\}^{1/2}$ -curvature parameter, $M = (\sigma B_0^2)/(\rho b)$ - magnetic parameter, $S = \alpha_1/b$ - unsteadiness parameter, $Pr = \nu/\alpha$ - Prandtl number, and $Ec = U^2/(C_p \Delta T)$ -Eckert number. Where $\Delta T = T_w - T_\infty$ is the temperature difference.

These physical quantities are the skin friction coefficient and wall heat transfer coefficient (Nusselt number) are given by:

$$C_f = \frac{2\tau_w}{\rho U^2} = \frac{2\mu \left(\frac{\partial w}{\partial r}\right)_{r=R}}{\rho U^2} = 2Re^{-1/2} f''(0) \quad (11)$$

$$Nu = \frac{Z\tau_w}{k(T_w - T_\infty)} = \frac{-zk \left(\frac{\partial T}{\partial r}\right)_{r=R}}{-T_{ref} \left(\frac{bz^2}{2v}\right) (1 - \alpha_1 t)^{-3/2}} = -kRe^{1/2} \theta'(0) \quad (12)$$

Where $Re = Uz/\nu$ is Reynolds number.

3. Numerical Results:

The non-linear ODEs, (8) and (9), together with the equation (7), are solved numerically, converting into an IVP (Initial value problem). Subsequently, an efficient numerical approach, namely *bvp4c* in MATLAB, is used for the computations. A new set of variables is defined as.

$$f = y(1), f' = y(2), f'' = y(3), \theta = y(4), \theta' = y(5)$$

So, the eqs. (4) and (5) take the form:

$$f''' = \frac{1}{1 + 2C\eta} \left\{ My(2) + Sy(2) + \frac{S\eta}{2} y(3) + [y(2)]^2 - 2Cy(3) - y(1)y(3) \right\} \quad (13)$$

$$\theta'' = \frac{1}{1 + 2C\eta} \left(-2Cy(5) - Pr \left\{ y(1)y(5) - 2y(2)y(4) - \frac{S}{2} [3y(4) + \eta y(5)] + (A^*y(2) + B^*y(4)) + Ec(1 + 2C\eta)[y(3)]^2 \right\} \right) \quad (14)$$

And related boundary conditions are:

$$\left. \begin{aligned} y(0) = 0, y(2) = 1, y(4) = 1 \\ y\beta(3) = 0, y\beta(5) = 0, y\beta(1) = \frac{S\beta}{2} \end{aligned} \right\} \quad (15)$$

The equations (8) and (9) include parameters: Unsteadiness parameter S, Curvature parameter C, Prandtl number Pr, magnetic parameter M, Eckert number Ec. The value for which $f(\beta) = \frac{S\beta}{2}$ holds is considered to be the suitable value for thickness of the film, and the IVP is solved by using the value of β .

4. Results and discussion:

Our research investigated behaviour of flow in boundary layer and the thermal profile of the fluid film over a cylinder undergoing unsteady stretching. We explored how various dimensionless factors influence the energy distribution and thermal boundary layer structure in presence of a magnetic field. By employing similarity transformations, we transformed the partial differential equations into dimensionless forms with different parameters. The numerical solutions were derived by the *bvp4c* method. We computed and tabulated the drag coefficient $f''(0)$, and local Nusselt number $\theta'(0)$, using predetermined the values of $M=1$, $C=0.5$, $S=0.8$, $Pr=0.7$, $Ec=0.5$, $A^*=0.5$ and $B^*=0.5$.

In Table 1, we compared numerical values for the skin friction coefficient and the Nusselt number across the different physical parameters. Our findings showed that increasing in the parameter S led to a rise in skin friction coefficient and a decline in Nusselt number, with magnetic parameter M fixed at 1 and the curvature parameter C at 0.5 as the film thickness β increased. Similarly, a higher magnetic parameter M resulted in an increased skin friction coefficient and a reduced Nusselt number for the fixed values of $S=0.8$ and $C=0.5$ with increasing film thickness β . Additionally, a greater curvature parameter C caused skin friction coefficient to increase and Nusselt number to decrease for fixed values of $S=0.8$ and $M=1$ with increasing film thickness β . When the Prandtl number (Pr) was increased for fixed values of $S=0.8$, $M=1$, $C=0.5$, and film thickness $\beta=1.8463774$, the skin friction coefficient converged to certain values while the Nusselt number decreased. Furthermore, a higher Eckert number (Ec) led to convergence of skin friction coefficient at certain values and an increase in Nusselt number.

Figure 2 illustrates the velocity profile $f'(\eta)$ influenced by the curvature parameter when S is 0.8 and M is 1. The results indicate that velocity increases with a higher curvature parameter C . This is attributed to the reduction in the cylinder's radius, resulting in less surface contact and lower resistance against fluid particles. Figure 3 shows the impacts of the magnetic parameter M on velocity profile $f'(\eta)$ when S is 0.8 and C is 0.5. An increase in magnetic parameter leads to a decrease in both the film thickness and velocity profile because the magnetic field produces Lorentz force which opposes the motion and hence decreases the motion.

Figures 4 and 5 analyze the effects of the unsteady parameter on velocity and temperature patterns for $M=1$ and $C=0.5$. The result reveals that an increase in unsteady parameter S leads to higher velocity and temperature fields, as S depends on α and b . This suggests that the stretching rate is crucial in determining the velocity profile's shape.

Figure 6 shows the effects of the Eckert number (Ec) on the temperature distribution $\theta(\eta)$ for $C = 0.5$, $S = 0.8$, $M = 1$, and $Pr = 0.7$. As Ec increases, the kinetic energy of the fluid particles rises, leading to an increase in the fluid's temperature. Figure 7 demonstrates the impacts of the Prandtl number (Pr) on temperature profile for $S = 0.8$, $M = 1$, $C = 0.5$, and $Ec = 0.5$. A higher Prandtl number results in a decrease in the fluid's temperature. This is because, the rate of heat transfer is restricted, leading to lower flow temperatures. Consequently, a higher Pr value indicates lower thermal conductivity in the fluid. The inverse relationship between the Pr and thermal diffusivity suggests that adjusting Prandtl number in conducting flows can enhance the fluid's thermal efficiency.

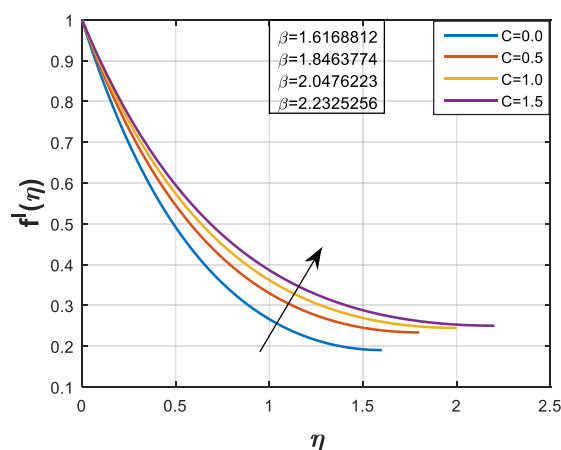
Figure 8 illustrates the impacts of the curvature parameter (C) on the temperature distribution for $S = 0.8$ and $M = 1$. The results indicate that an increase in C leads to higher velocity, increasing kinetic

energy and subsequently raising the temperature. The magnetic field exerts a Lorentz force on the electrically conducting fluid, acting as a resistive force that reduces the fluid's velocity. This applied magnetic field also induces polarization and dipole formation in the fluid, resulting in a decreased flow rate.

Figures 9 and 10 depict the influence of varying heat source/sink parameters on the temperature distribution $\theta(\eta)$. The results show that an increase in the values A^* and B^* leads to a rise in fluid temperature. Increasing the irregular heat source/sink parameters generates more heat within the flow. The higher fluid temperatures are associated with the values of A^* and B^* .

Table 1. Comparison of numerical values of $-f''(0)$ and $-\theta'(0)$ for different values of S, M, C, β, Pr and Ec .

| S | M | C | β | Pr | Ec | Azeem et. Al.[22] | | Present Results | |
|-----|---|-----|-----------|-----|-----|-------------------|-----------|-----------------|-----------|
| | | | | | | $-\theta'(0)$ | $-f''(0)$ | $-\theta'(0)$ | $-f''(0)$ |
| 0.4 | | | 4.2215372 | | | -2.8207767 | 1.7277173 | -2.866379 | 1.707085 |
| 0.8 | 1 | 0.5 | 1.8463774 | | | -3.3104618 | 1.7771620 | -2.869634 | 1.656843 |
| 1.0 | | | 1.3389099 | | | -3.6047990 | 1.7617442 | -3.028029 | 1.583077 |
| | 0 | | 2.5658506 | | | -3.7423303 | 1.4242913 | -3.686028 | 1.252673 |
| 0.8 | 1 | 0.5 | 1.8463774 | 0.7 | | -3.3104618 | 1.7771620 | -2.815867 | 1.561332 |
| | 2 | | 1.5098493 | | | -2.9387683 | 2.0630116 | -2.500338 | 1.816044 |
| | | 0 | 1.6168812 | | 0.5 | -3.2908687 | 1.5893922 | -3.719899 | 1.534623 |
| 0.8 | 1 | 0.5 | 1.8463774 | | | -3.3104618 | 1.7771620 | -3.169512 | 1.561332 |
| | | 1 | 2.0476223 | | | -3.3478826 | 1.9464131 | -2.834221 | 1.544100 |
| | | | | 2 | | -2.0626625 | - | -1.778244 | 1.561332 |
| | | | | 4 | | -2.7902466 | - | -2.320936 | 1.561332 |
| 0.8 | 1 | 0.5 | 1.8463774 | 6 | | -3.3104618 | - | -2.672900 | 1.561332 |
| | | | | 2 | 0 | -4.5342481 | - | -3.751095 | 1.561331 |
| | | | | 4 | 0.5 | -3.3104618 | - | -2.320936 | 1.561332 |
| | | | | 6 | 1 | -2.0866755 | - | -1.594574 | 1.561334 |



3 Figure 2: Impact of Curvature parameter on velocity profile $f'(\eta)$

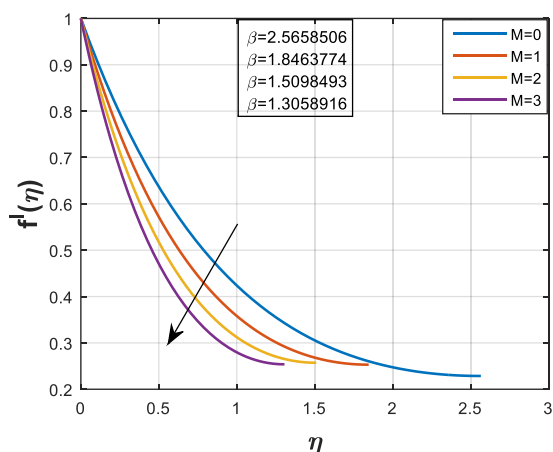


Figure 3: Impact of Magnetic parameter on velocity profile $f'(\eta)$

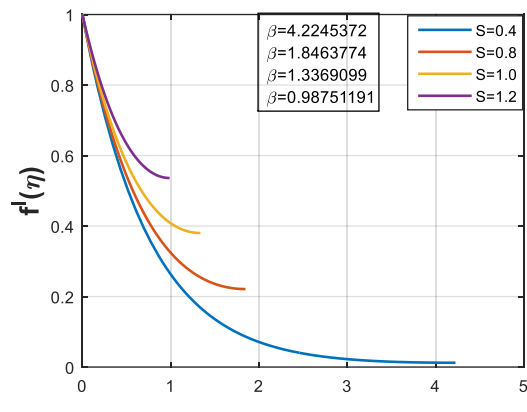


Figure 4: Impact of unsteadiness parameter on velocity profile $f'(\eta)$

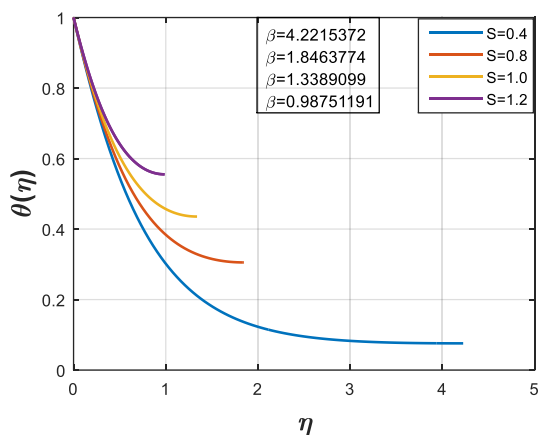


Figure 5: Impact of unsteadiness parameter on Temperature profile $\theta(\eta)$

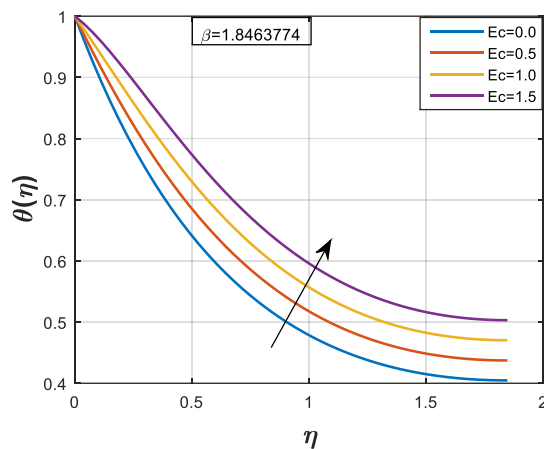


Figure 6: Impact of Eckert number on Temperature profile $\theta(\eta)$

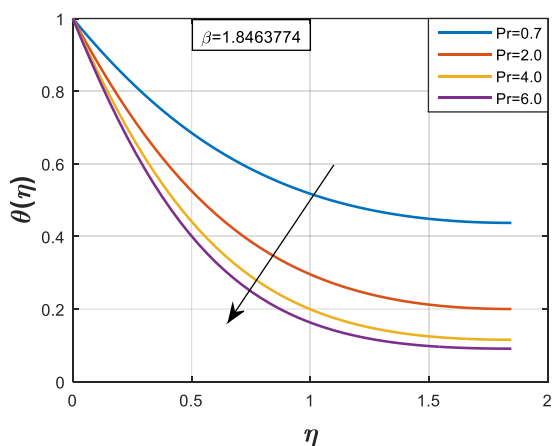


Figure 7: Impact of Prandtl number on Temperature profile $\theta(\eta)$

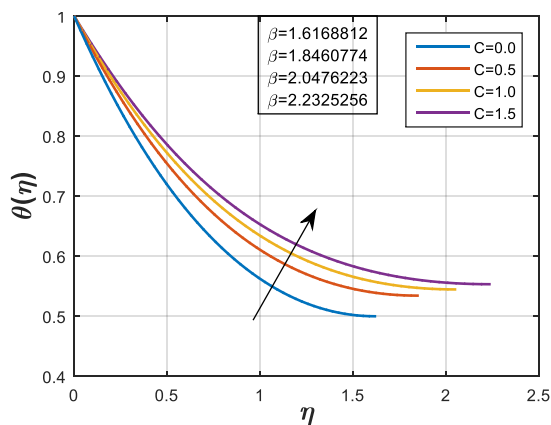


Figure 8: Impact of Curvature parameter on Temperature profile $\theta(\eta)$

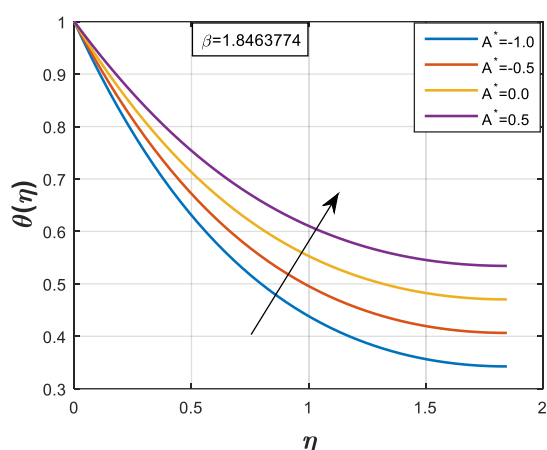


Figure 9: Impact of A^* on Temperature profile $\theta(\eta)$

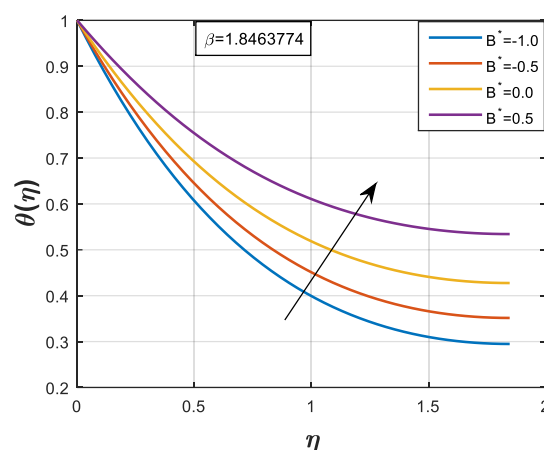


Figure 10: Impact of B^* on Temperature profile $\theta(\eta)$

5. Conclusion:

The current study investigates the influence of a magnetic field and variable heat source/sink on the flow and the thermal transport of a viscous fluid along a stretched cylinder, specifically focusing on the axisymmetric thin film. An analysis is conducted to investigate the impact of several dimensionless characteristics, which are then visually shown. In addition, the tabular format provides an assessment of *skin friction coefficient* and *Nusselt number values*. The following findings have been obtained.

- By increasing the curvature parameter, there is a noticeable increase in both temperature and velocity profiles.
- The increasing estimates of the unsteady parameter describe the rise in velocity and temperature profiles whereas decreases the fluid viscosity.
- The Eckert number is to decrease the Nusselt number.
- Increased A^* and B^* values lead to fluid temperature enrichment within the boundary region.
- The skin friction coefficient improves due to the rise in the unsteadiness, curvature, and magnetic parameters. Meanwhile, the Nusselt number increases with an increase in the Prandtl number and curvature parameter.

References:

- [1] Partha Pratim Gogoi and Susanta Maity., Thermocapillary thin film flow upon a porous heated stretchable cylinder., *Heat Transfer* 2024;53:73–96.
- [2] Alabduhadi S, Abu Bakar S, Ishak A, Waini I, Ahmed SE. Effect of Buoyancy Force on an Unsteady Thin Film Flow of Al₂O₃/Water Nanofluid over an Inclined Stretching Sheet. *Mathematics*. 2023; 11(3):739. <https://doi.org/10.3390/math11030739>
- [3] Yan Zhang, Min Zhang, Shujuan Qi, Heat and Mass Transfer in a Thin Liquid Film over an Unsteady Stretching Surface in the Presence of Thermosolutal Capillarity and Variable Magnetic Field., *Mathematical Problems in Engineering*., Volume 2016 <https://doi.org/10.1155/2016/8521580>
- [4] K. Vajravelu, K.V. Prasad, Chiu-On Ng, Unsteady flow and heat transfer in a thin film of Ostwald–de Waele liquid over a stretching surface., *Communication in Nonlinear Science and Numerical Simulation* Volume 17, Issue 11, <https://doi.org/10.1016/j.cnsns.2012.01.027>
- [5] Ziad Khan, Rashid Jan, Muhammad Jawad, Fawad Hussain. Radiation heat transfer of hybrid nanofluid stagnation point flow across a stretching porous cylinder., *Thermal Science and Engineering* 2595 Vol 6, Issue 2, 2023.
- [6] Hayat, Umer, Ramzan Ali, Shakil Shaiq and Azeem Shahzad. A numerical study on thin film flow and heat transfer enhancement for copper nanoparticles dispersed in ethylene glycol. *Reviews on advanced materials science*., 62 (2023): n. pag.

- [7] Azeem Shahzad, Uzma Gulistan, Ramzan Ali, Azhar Iqbal, Ali Cemal Benim, Muhammad Kamran, Salah Ud-Din Khan, Shahab Ud-Din Khan, and Aamir Farooq. Numerical Study of Axisymmetric Flow and Heat Transfer in a Liquid Film over an Unsteady Radially Stretching Surface., *Mathematical Problems in Engineering* Volume 2020, Article ID 6737243, 9 pages. <https://doi.org/10.1155/2020/6737243>
- [8] Khan W and Gul T. The Thin Film Flow of Walter's B Fluid over the Surface of a Stretching Cylinder with Heat and Mass Transfer Analysis *Journal of Applied & Computational Mathematics* Volume 7. Issue 3. doi: 10.4172/2168-9679.1000411
- [9] Mostafa A. A. Mahmoud and Ahmed M. Megahed MHD flow and heat transfer in a non-Newtonian liquid film over an unsteady stretching sheet with variable fluid properties. *Canadian Journal of Physics* Volume 87, Number 10, <https://doi.org/10.1139/P09-066>.
- [10] Waheed, S.E. Flow and heat transfer in a Maxwell liquid film over an unsteady stretching sheet in a porous medium with radiation. *Springer Plus* 5, 1061 (2016). <https://doi.org/10.1186/s40064-016-2655-x>.
- [11] Shikha Kandwal, Ashish Mishra, Manoj Kumar numerical investigation of nanofluid heat transfer in an inclined stretching cylinder under the influence of suction/ injection and viscous dissipation *Nanoscience and Technology: An International Journal* Volume 10, 2019 Issue 1 DOI: 10.1615/NanoSciTechnolIntJ.2018026365.
- [12] Gomathy, G., & Rushi Kumar, B. (2024). Thin film flow dynamics and heat transfer enhancement in porous media: Shape-dependent behavior of Al₂O₃ nanoparticles. *Numerical Heat Transfer, Part A: Applications*, 1–18. <https://doi.org/10.1080/10407782.2024.2304063>.
- [13] Tawade JV, Biradar MM, Dakshayini N, B M. Analysis of volume fraction of Casson Nanofluid flow over a flat moving plate with thermal radiation and nonuniform heat source/sink. *J. Int. Acad. Phys. Sci* 27(3):259-74. <https://www.iaps.org.in/journal/index.php/journaliaps/article/view/998>.
- [14] Gamal and Abdel-Rahman Effect of Magnetohydrodynamic on Thin Films of Unsteady Micropolar Fluid through a Porous Medium. *Journal of Modern Physics* Vol.2 No.11, DOI: 10.4236/jmp.2011.211160.
- [15] Alshehry, Azzh Saad, Yasmin, Humaira and Shah, Rasool. "3D thin-film nanofluid flow with heat transfer on an inclined disc by using HWCM" *Open Physics*, vol. 21, no. 1, 2023, pp. 20230122. <https://doi.org/10.1515/phys-2023-0122>.
- [16] Govindasamy G, Bangalore RK. Heat and mass transfer in thin film flow of Casson nanofluid over an unsteady stretching sheet. *Proceedings of the Institution of Mechanical Engineers, Part E: Journal of Process Mechanical Engineering*. 2023;0(0). doi:10.1177/09544089221150727.
- [17] Mohammed Ali and Md. Abdul Alim Numerical Analysis of Boundary Layer Flow and Heat Transfer over a Stretching and Non-Stretching BulletShaped Object., *Athens Journal of Sciences-* Volume 8, Issue 4,
- [18] Muhammad Jawad and Zahir Shah and Saeed Islam and Ebenezer Bonyah and Aurang Zeb Khan Darcy-Forchheimer flow of MHD nanofluid thin film flow with Joule dissipation and Navier's partial slip *Journal of Physics Communications* Volume 2. DOI 10.1088/2399-6528/aaeddf.
- [19] Hayat, Umer; Ali, Ramzan; Shaiq, Shakil; Shahzad, Azeem. A numerical study on thin film flow and heat transfer enhancement for copper nanoparticles dispersed in ethylene glycol. *Manara - Qatar Research Repository. Journal contribution*. 2023 <https://doi.org/10.1515/rams-2022-0320>.
- [20] Yan Zhang, Min Zhang, Yu Bai., Unsteady flow and heat transfer of power-law nanofluid thin film over a stretching sheet with variable magnetic field and power-law velocity slip effect., *Journal of the Taiwan Institute of Chemical Engineers* Volume 70 <https://doi.org/10.1016/j.jtice.2016.10.052>
- [21] Miran, S. and Sohn, C.H. (2015), "Numerical study of the rounded corners effect on flow past a square cylinder", *International Journal of Numerical Methods for Heat & Fluid Flow*, Vol. 25 No. 4, pp. 686-702. <https://doi.org/10.1108/HFF-12-2013-0339>
- [22] Shahzad, A., Habib, B., Nadeem, M., Kamran, M., Ahma, H., Atif, M., & Ahmad, S. (2021). Numerical analysis of flow and heat transfer in a thin film along an unsteady stretching cylinder. *Thermal Science*, 25(Spec. issue 2), 441-448.
- [23] Anantha Kumar, K., Sandeep, N., Sugunamma, V. et al. Effect of irregular heat source/sink on the radiative thin film flow of MHD hybrid ferrofluid. *J Therm Anal Calorim* 139, 2145–2153 (2020). <https://doi.org/10.1007/s10973-019-08628-4>.

- [24] Giri, S.S., Das, K. and Kundu, P.K. (2019), "Inclined magnetic field effects on unsteady nanofluid flow and heat transfer in a finite thin film with non-uniform heat source/sink", *Multidiscipline Modeling in Materials and Structures*, Vol. 15 No. 1, pp. 265-282. <https://doi.org/10.1108/MMMS-04-2018-0065>.
- [25] Khan NS, Gul T, Islam S, Khan I, Alqahtani AM, Alshomrani AS. Magnetohydrodynamic Nanoliquid Thin Film Sprayed on a Stretching Cylinder with Heat Transfer. *Applied Sciences*. 2017; 7(3):271. <https://doi.org/10.3390/app7030271>.
- [26] T. Hayat, M. Sajid, On analytic solution for thin film flow of a fourth grade fluid down a vertical cylinder, *Physics Letters A*, Volume 361, Issues 4–5, 2007, Pages 316-322, <https://doi.org/10.1016/j.physleta.2006.09.060>.
- [27] Ross Ab, Wilson Sk, Duffy Br. Thin-Film Flow of a Viscoplastic Material Round a Large Horizontal Stationary or Rotating Cylinder. *Journal of Fluid Mechanics*. 2001;430:309-333. Doi:10.1017/S0022112000002974

Nomenclature:

| | |
|-----------------|---|
| u, w | Velocity components in x and y-direction [ms^{-1}] |
| ν | Kinematic viscosity [m^2s^{-1}] |
| q''' | Non-Uniform Heat source/sin [Ks^{-1}] |
| σ | Electrical conductivity [Sm^{-1}] |
| B^2 | Magnetic field [T] |
| ρ | Fluid density [$gm^{-1}l^{-1}$] |
| u_w, u_∞ | Velocity at the near and far away from the surface |
| α | Thermal diffusivity [m^2S^{-1}] |
| ρC_p | Heat capacity of the Fluid [$Jkg^{-1}K^{-1}$] |
| τ | Fraction of heat capability of nanofluid |
| T_w, T_∞ | Temperature at the near and far away from the surface |
| μ | Dynamic viscosity of the fluid [$kgm^{-1}s^{-1}$] |
| c_p | Specific heat at constant pressure [$Jkg^{-1}K^{-1}$] |
| α_l, b | Constant parameters |
| T | Temperature of the fluid [K] |
| M | Magnetic field parameter [T] |
| C | Curvature Parameter |
| Pr | Prandtl number |
| Ec | Eckert number |
| S | Unsteadiness parameter |
| A^*, B^* | Non-Uniform Heat source/sink |
| C_f | Skin friction co-efficient |
| q_w | Wall Heat flux [Wm^{-2}] |
| Re | Local Reynolds number |
| Nu | Local R Nusselt number s number |